



ARL-TN-0964 • SEP 2019



# Microstructural Texturing of Silicon Nitride for Propulsion Applications Using a Magnetic Field

by John J Pittari III and Stephen C Bady

Approved for public release; distribution is unlimited.

## **NOTICES**

### **Disclaimers**

The findings in this report are not to be construed as an official Department of the Army position unless so designated by other authorized documents.

Citation of manufacturer's or trade names does not constitute an official endorsement or approval of the use thereof.

Destroy this report when it is no longer needed. Do not return it to the originator.



# **Microstructural Texturing of Silicon Nitride for Propulsion Applications Using a Magnetic Field**

**by John J Pittari III**

*Weapons and Materials Research Directorate, CCDC Army Research Laboratory*

**Stephen C Bady**

*Drexel University*

**REPORT DOCUMENTATION PAGE**

*Form Approved  
OMB No. 0704-0188*

Public reporting burden for this collection of information is estimated to average 1 hour per response, including the time for reviewing instructions, searching existing data sources, gathering and maintaining the data needed, and completing and reviewing the collection information. Send comments regarding this burden estimate or any other aspect of this collection of information, including suggestions for reducing the burden, to Department of Defense, Washington Headquarters Services, Directorate for Information Operations and Reports (0704-0188), 1215 Jefferson Davis Highway, Suite 1204, Arlington, VA 22202-4302. Respondents should be aware that notwithstanding any other provision of law, no person shall be subject to any penalty for failing to comply with a collection of information if it does not display a currently valid OMB control number.

**PLEASE DO NOT RETURN YOUR FORM TO THE ABOVE ADDRESS.**

<b>1. REPORT DATE (DD-MM-YYYY)</b> September 2019		<b>2. REPORT TYPE</b> Technical Note		<b>3. DATES COVERED (From - To)</b> 1 April 2016–1 July 2019	
<b>4. TITLE AND SUBTITLE</b> Microstructural Texturing of Silicon Nitride for Propulsion Applications Using a Magnetic Field				<b>5a. CONTRACT NUMBER</b>	
				<b>5b. GRANT NUMBER</b>	
				<b>5c. PROGRAM ELEMENT NUMBER</b>	
<b>6. AUTHOR(S)</b> John J Pittari III and Stephen C Bady				<b>5d. PROJECT NUMBER</b>	
				<b>5e. TASK NUMBER</b>	
				<b>5f. WORK UNIT NUMBER</b>	
<b>7. PERFORMING ORGANIZATION NAME(S) AND ADDRESS(ES)</b> CCDC Army Research Laboratory ATTN: FCDD-RLW-MB Aberdeen Proving Ground, MD 21005				<b>8. PERFORMING ORGANIZATION REPORT NUMBER</b>  ARL-TN-0964	
<b>9. SPONSORING/MONITORING AGENCY NAME(S) AND ADDRESS(ES)</b>				<b>10. SPONSOR/MONITOR'S ACRONYM(S)</b>	
				<b>11. SPONSOR/MONITOR'S REPORT NUMBER(S)</b>	
<b>12. DISTRIBUTION/AVAILABILITY STATEMENT</b> Approved for public release; distribution is unlimited.					
<b>13. SUPPLEMENTARY NOTES</b> *The work outlined in this report was performed while the US Army Research Laboratory (ARL) was part of the US Army Research, Development, and Engineering Command (RDECOM). As of 1 February 2019, the organization is part of the US Army Combat Capabilities Development Command (formerly RDECOM) and is now called CCDC Army Research Laboratory. ORCID ID(s): John J Pittari, 0000-0001-9611-3138					
<b>14. ABSTRACT</b> In recent years, the interest in employing silicon nitride (Si <sub>3</sub> N <sub>4</sub> ) ceramics in propulsion applications has grown immensely due to its ideal combination of high-temperature properties and tribological behavior. However, its brittle nature promotes concern when used as critical components in certain applications. The development of microstructural texturing through alignment of the c-axis of the β grains has been shown to improve the properties of the ceramic parts. Further advances in this area may further increase the utilization of Si <sub>3</sub> N <sub>4</sub> as propulsion components. This study aims to produce Si <sub>3</sub> N <sub>4</sub> bodies with microstructural texturing developed through alignment in a magnetic field. Proof-of-concept experiments where Si <sub>3</sub> N <sub>4</sub> is aligned in epoxy were produced initially. Once densified, a detailed microstructural analysis was conducted along with density, hardness, and relative toughness evaluations. X-ray diffraction was used to determine the degree of orientation in the cast bodies. Final bodies were produced through slip- or gel-casting techniques. In addition, these bodies underwent tribological and thermal cycling tests. However, the strength of the magnet available for this investigation was limited to 2T, which is well below the value required to achieve large-scale alignment, which limited the results of the study. These results are presented and discussed along with the problems encountered. Recommendations for improving future efforts in this effort are presented.					
<b>15. SUBJECT TERMS</b> silicon nitride, microstructure, texturing, alignment, slip-casting					
<b>16. SECURITY CLASSIFICATION OF:</b>			<b>17. LIMITATION OF ABSTRACT</b>  UU	<b>18. NUMBER OF PAGES</b>  25	<b>19a. NAME OF RESPONSIBLE PERSON</b> John J Pittari III
<b>a. REPORT</b> Unclassified	<b>b. ABSTRACT</b> Unclassified	<b>c. THIS PAGE</b> Unclassified			<b>19b. TELEPHONE NUMBER (Include area code)</b> (410) 306-0773

## Contents

---

<b>List of Figures</b>	<b>iv</b>
<b>List of Tables</b>	<b>iv</b>
<b>Acknowledgments</b>	<b>v</b>
<b>1. Introduction</b>	<b>1</b>
<b>2. Material</b>	<b>2</b>
<b>3. Experimental Procedure</b>	<b>3</b>
<b>4. Results and Conclusions</b>	<b>5</b>
4.1 Experimental Results	5
4.2 Problems Encountered	6
4.2.1 Magnet Strength	7
4.2.2 Starting Powder Morphology	7
4.2.3 Anisotropic Magnetic Susceptibility of Silicon Nitride	8
<b>5. Future Efforts</b>	<b>9</b>
5.1 Magnetic Field Considerations	9
5.2 Starting Powders	9
5.3 Alternative Processing Methods	10
5.4 Controlling Grain Orientation for Specific Applications	12
<b>6. References</b>	<b>14</b>
<b>List of Symbols, Abbreviations, and Acronyms</b>	<b>17</b>
<b>Distribution List</b>	<b>18</b>

## List of Figures

---

Fig. 1	Microstructure of a $\beta$ - $\text{Si}_3\text{N}_4$ showing the elongated, whisker-like grains that can be utilized to improve crack resistance. ....	3
Fig. 2	Molding cup and produced sample with the sectioning line. The shown angle of the sectioning line is not representative of the aforementioned sectioning axis.....	4
Fig. 3	SEM image of the initial $\text{Si}_3\text{N}_4$ powder .....	8
Fig. 4	a) Schematic of the hexagonal crystal of $\beta$ silicon nitride grains with the major axes noted. b) Schematic of how the anisotropic magnetic susceptibility of $\beta$ -silicon nitride grains affects the alignment after a magnetic field has been imposed. Because the c-axis susceptibility is below that of the a- and b-axes in silicon nitride, the particles will only align in the same plane, but not along the same direction. ....	9
Fig. 5	Rotation of grains due to a) hot-working and b) templated grain growth. In hot-working, the grains are aligned due to the pressing forces applied during processing; however, in templated grain growth, seed grains are aligned and then proceed to grow epitaxially during sintering to produce the large-scale microstructural texturing. ....	10
Fig. 6	Illustrations showing how a) extrusion and b) tape casting can be utilized to produce green bodies with microstructural texturing of $\beta$ silicon nitride grains. In extrusion, the particles are aligned in the same direction; however, in tape casting, the particles will lie in the same plane but not all pointing in the same direction.....	11
Fig. 7	Illustration of how 3-D magnetic printing can be used to produce ceramics with highly controllable microstructural texturing. Through selective sintering and alignment procedures, different regions or layers of material can be oriented in their own independent direction, resulting in a material with an enhanced, but exceedingly controlled, microstructural texturing. ....	13

## List of Tables

---

Table 1	Results of the Lotgering factor calculations for each of the materials produced in this investigation .....	6
---------	---	---

## **Acknowledgments**

---

The research efforts of John Pittari III were supported in part by an appointment to the Postgraduate Research Participation Program at the CCDC Army Research Laboratory (ARL) administered by the Oak Ridge Institute for Science and Education through an interagency agreement between the US Department of Energy and ARL. The efforts of Stephen Bady were supported by the ARL College Qualified Leaders program administered by The Academy of Applied Sciences.

## 1. Introduction

---

Silicon nitride ( $\text{Si}_3\text{N}_4$ ) is an important ceramic material for a vast array of applications due to its low density ( $3.2 \text{ g/cm}^3$ ),<sup>1,2</sup> high hardness ( $>15 \text{ GPa}$ ),<sup>3-8</sup> high fracture toughness ( $>6 \text{ MPa}\sqrt{\text{m}}$ ),<sup>4,9-17</sup> and good tribological properties, among others.<sup>1,2</sup> Additionally,  $\text{Si}_3\text{N}_4$  has excellent high-temperature strength, low thermal expansion, and exhibits good oxidation and corrosion resistance.<sup>1-3,18</sup> This combination of attributes makes it an ideal candidate for applications in the automotive industry as gasoline and diesel engine components, where improvement upon the properties and behavior of common metallic parts is of immense interest. More recently, due to reductions in production costs,  $\text{Si}_3\text{N}_4$  is being used in both full ceramic and ceramic hybrid bearings because it is harder than steel, exhibits excellent thermal shock and wear resistance, and allows for weight reduction due to its low density.  $\text{Si}_3\text{N}_4$  can operate under lubrication starvation and at higher operating temperatures than steels, increasing its appeal to the aerospace industry, where high-temperature performance is of utmost concern. Further, in environments where corrosion and electric/magnetic fields may compromise the integrity of metal bearing systems,  $\text{Si}_3\text{N}_4$  is an excellent alternative. Though  $\text{Si}_3\text{N}_4$  bearings remain two-to-five times more expensive than high-end steel bearings, their superior performance and extended usage life justify adoption. Unfortunately, like most ceramics,  $\text{Si}_3\text{N}_4$  is inherently brittle, limiting its usefulness in some high-temperature applications. Research is ongoing within the ceramics community to develop stronger and tougher ceramics through grain boundary engineering, microstructural tailoring, and incorporating second phase materials to create ceramic matrix composites.

Over the years, the US Army has supported the investigation and development of  $\text{Si}_3\text{N}_4$  as a bearing and gear material for the hot sections in diesel and gas turbine engines and as a gun barrel liner. There is a strong interest in the US Army Combat Capabilities Development Command Army Research Laboratory's Vehicle Technology Directorate to develop stronger and tougher  $\text{Si}_3\text{N}_4$  materials for rotorcraft applications. One such interest is developing an all-ceramic bearing and geared system to reduce friction, increase bearing and gear life and operating temperature and speed, reduce weight, and have the ability to operate in a lubrication-starved environment. Subsequent research by Ceradyne<sup>19-22</sup> to develop an  $\text{Si}_3\text{N}_4$  material for use as a gun barrel liner confirmed the role of the rare-earth oxides in the development and growth of  $\beta$  grains and the associated improvement in properties. They identified a combination of lanthanum oxide and lutetium oxide as the most promising for high strength and fracture toughness.

The approach for the current investigation was intended to be very simplistic and straightforward. The products of this investigation were anticipated to be a proof of concept to spark further interest and a more comprehensive investigation into the formation of these microstructurally textured silicon nitrides. The overall goal was to achieve the grain orientation through slip- or gel-casting of a slurry containing suspended  $\text{Si}_3\text{N}_4$  ceramic particles that would be placed in a static magnetic field for alignment throughout the casting duration. Some specimens were densified in a furnace. All specimens were microstructurally analyzed through X-ray diffraction (XRD) and scanning electron microscopy (SEM) techniques to observe and attempt to quantify the degree of alignment. Density, microhardness, and indentation toughness were investigated to understand basic mechanical properties of the specimens. When the results were found to be extremely promising, specimens underwent application-specific testing, such as tribological testing and thermal cycling, as well as characterization of the surface wear and subsurface damage degradation.

## 2. Material

---

There are three distinct crystallographic structures in which  $\text{Si}_3\text{N}_4$  can exist, designated as alpha ( $\alpha$ ), beta ( $\beta$ ), and gamma ( $\gamma$ ). The  $\alpha$ -phase (trigonal) and  $\beta$ -phase (hexagonal) are the most common forms and can be produced under normal pressure conditions. The  $\gamma$ -phase (cubic) is harder (35 GPa) than the other two phases but can only be synthesized under extreme temperatures and pressures.<sup>23</sup> The  $\beta$ -phase has the lowest hardness of the three phases but is chemically stable compared with the  $\alpha$ -phase, which readily (i.e., always) transforms into the  $\beta$ -phase at high temperature under the presence of a liquid phase.<sup>3</sup> Therefore,  $\beta$ -silicon nitride is the main form used in monolithic ceramics, such as in the microstructure shown in Fig. 1.

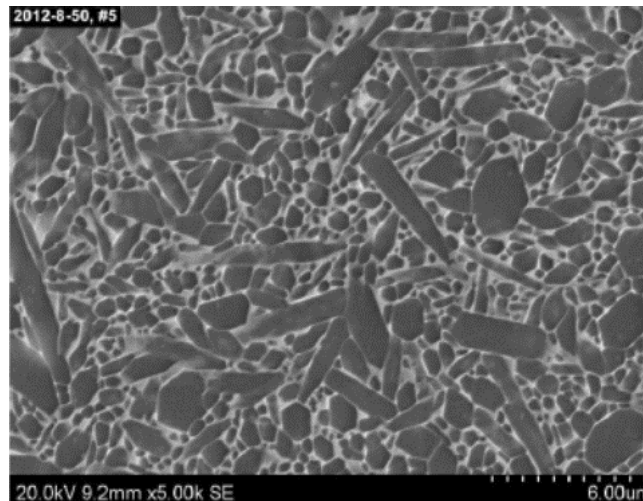


**Fig. 1** Microstructure of a  $\beta$ - $\text{Si}_3\text{N}_4$  showing the elongated, whisker-like grains that can be utilized to improve crack resistance. (Reprinted use with permission from Mikijelj et al.<sup>19</sup>)

The hexagonal crystal structure of  $\beta$ -phase  $\text{Si}_3\text{N}_4$  produces an anisotropic magnetic susceptibility, meaning that the grains can be rotated and, potentially, aligned.<sup>18,24</sup> This previous research indicated that under a strong field ( $>6$  T) the  $\beta$  grains can be rotated during initial processing. This orientation is maintained and developed during the densification phase, leading to a material with higher strength and, potentially, greater toughness. Various rare-earth oxides have been shown to have an influence on the microstructure of  $\text{Si}_3\text{N}_4$ , such as promotion of the  $\alpha$ -to- $\beta$  phase transformation, densification, and grain growth of  $\beta$ -silicon nitride.<sup>3,4,25–27</sup> Research has also shown that these oxides have a tremendous impact on the strength and fracture toughness.  $\text{Si}_3\text{N}_4$  materials with strength greater than 1 GPa and fracture toughness greater than  $10 \text{ MPa}\sqrt{\text{m}}$  have been reported.<sup>27</sup> These oxides promote the  $\alpha$ -to- $\beta$  transformation in  $\text{Si}_3\text{N}_4$ , which leads to greater anisotropy of the  $\beta$  grains, resulting in elongated grains with higher aspect ratio.

Many anisotropic properties can be influenced by grain orientation, such as hardness, elastic modulus, flexure strength, fracture toughness, tribological and wear resistance, contact damage resistance, and thermal conductivity.<sup>3</sup> All of these properties are what make  $\text{Si}_3\text{N}_4$  an ideal candidate for propulsion applications. Furthermore, microstructurally tailored  $\text{Si}_3\text{N}_4$  with specifically oriented grains could be a crucial performance improvement in applications where load directionality is a big consideration, such as for bearing raceways and engine components. Therefore, the objective of this research is to determine if developing texturing in an  $\text{Si}_3\text{N}_4$  ceramic, through the application of a magnetic field, will lead to a material with improved strength and fracture toughness that could be employed in propulsion applications.

### **3. Experimental Procedure**

---

To understand the effect of processing without going through a rigorous optimization study of the  $\text{Si}_3\text{N}_4$  slurry, including dispersants and sintering additives, initial alignment experiments were performed by aligning  $\text{Si}_3\text{N}_4$  particles in a two-part epoxy. This allows for isolation of the alignment procedure of the grains from the effects of the slurry chemistry on the casting procedure and mold material/technique. For these experiments, commercially available  $\text{Si}_3\text{N}_4$  powder was acquired ( $-325$  mesh, 99.7%  $\beta$ - $\text{Si}_3\text{N}_4$ ). The powder was dispersed in methanol at 20% solids loading by weight, using a resonant acoustic mixer at 30% intensity for 5 min. Following this procedure, 5 g of part A of a two-part epoxy was combined with this slurry via a magnetic stir bar and plate. The methanol was allowed to

evaporate, leaving the  $\text{Si}_3\text{N}_4$  dispersed in part A of the epoxy. This mixture was combined with part B in the manufacturer's recommended ratio and then cast in plastic cups (25-mm diameter by ~12 mm height). (Since there would be no sintering component at this stage of the experiment, only two samples were cast.) The sample for alignment was then immediately placed within the pole pieces of the magnet and allowed to cure. The sample was cut in a fashion both along the axis of and parallel to the plane of the pole pieces. Alignment was investigated using XRD along the cut surface. An image of the mold and cured sample with the sectioning line is shown in Fig. 2.



**Fig. 2** Molding cup and produced sample with the sectioning line. The shown angle of the sectioning line is not representative of the aforementioned sectioning axis.

Two different epoxies were investigated, referred to as soft and hard. The soft epoxy had a shorter cure time and resulted in a rubber-like consistency when cured, while the hard epoxy had a longer cure time and was more rigid in its cured state. This allowed for an investigation of the relationship between magnetic exposure time and achieved orientation.

For the slip- and gel-casting procedures, three specimens were to be produced in each batch: 1) control specimen (C), 2) aligned specimen (A), and 3) aligned and sintered specimen (AS). The control specimen was placed in the same environment as the two specimens that were placed in the magnetic field for alignment, but not within range of the magnetic field. This was in an effort to isolate the effects of the magnetic alignment from any other background fields in the same environment. It is understood that sintering induces a further degree of alignment beyond that of just the magnetic field.<sup>24</sup> Therefore, the third sample was to be used to investigate the effect of sintering upon further alignment.

There are numerous analytical methods to quantify the degree of alignment of a material via XRD with varying degrees of complexity, including Lotgering factor, relative peak intensities, orientation indices, relative facial angle, pole figure, XRD rocking curve, and Reitveld refinement.<sup>3</sup> (Other methods for analyzing alignment include SEM image analysis and electron backscatter detection.) The Lotgering factor ( $LF$ ) was the preferred method for this investigation due to its simplicity and rapid results.<sup>28</sup> The value of  $LF$  varies between 0 and 1, where a value of 0 corresponds to random orientation while a value of unity represents perfect orientation. (Therefore, the value of  $LF$  can be considered a percentage of obtained alignment.) The  $LF$  is calculated as a ratio of XRD peak intensities and is defined as

$$LF = \frac{(P-P_0)}{(1-P_0)}, \quad (1)$$

where  $P$  is the fraction of the summation of the peak intensities corresponding to the preferred orientation axis to that of the summation of all diffraction peaks in particle-oriented materials, and  $P_0$  is a singular value of  $P$  for a material with a random particle orientation. Therefore, the values of  $P$  are obtained from the sample, while the values of  $P_0$  are obtained from the standard powder diffraction file (PDF) card (No. 33-1160) for  $\beta$ -silicon nitride. Due to the symmetry of the a- and b-axes in  $\beta$ -silicon nitride, the  $P$  and  $P_0$  values can be represented as

$$P, P_0 = \frac{\Sigma I_{(hk0)}}{\Sigma I_{(hkl)}}. \quad (2)$$

For c-axis orientation, the  $P$  and  $P_0$  values are calculated as

$$P, P_0 = \frac{\Sigma I_{(00l)}}{\Sigma I_{(hkl)}}. \quad (3)$$

In Eqs. 2 and 3,  $\Sigma I_{(hk0)}$  and  $\Sigma I_{(00l)}$  are the sums of the peak intensities of the  $(hk0)$  and  $(00l)$  planes parallel and perpendicular to the c-axis of the  $\beta$ -silicon nitride crystal, respectively, and  $\Sigma I_{(hkl)}$  is the sum of the peak intensities of all the  $(hkl)$  planes in the range of  $2\theta$ . There are some issues with this method, however, and it is therefore only considered to be semi-quantitative. This was considered adequate for the adolescent nature of this investigation.

## 4. Results and Conclusions

---

### 4.1 Experimental Results

---

Four samples of  $\beta$ -silicon nitride powders cast in epoxy were produced using the aforementioned procedure. Two samples were cast in a soft epoxy, while another

pair were cast in a harder epoxy. The samples were bisected along the axis of the magnet pole pieces in a plane parallel to the magnetic field. XRD analysis was then performed on this face of the sample, and the peak intensities were tabulated and the calculations for the  $LF$  were performed. To evaluate the validity of the control samples, their  $LF$  values were compared with the PDF card values. The results of all the experiments are presented in Table 1.

**Table 1 Results of the Lotgering factor calculations for each of the materials produced in this investigation**

Sample comparison	Soft epoxy		Hard epoxy	
	$LF_{a,b}$	$LF_c$	$LF_{a,b}$	$LF_c$
C vs. PDF	0.08	0.00	0.10	0.00
A vs. PDF	0.11	0.00	0.06	0.00
A vs. C	0.03	0.00	0.04	0.00

Notes: C = control specimen; A = aligned specimen

Overall, minimal alignment (<11%) was noted in all of the samples. The highest values of a- and b-axis alignment were noted between the control and aligned samples with the PDF card values, while the aligned and control samples exhibited less than 4% alignment when compared directly. This indicates that the control samples were not fully isolated from the magnetic field even though their locations were checked with a probe. Particle settling during curing may have also resulted in low levels of microstructural texturing. However, there may have been external fields in the experimental area affecting the results of this study. Absolutely no alignment in the c-axis direction was noted for all of the samples. All of the poor results are attributed to the weakness of the magnetic field. The magnetic used for this investigation was capable of reaching a maximum field strength of 2 T. This value decreases with increasing distance between the pole pieces; therefore, samples with a small diameter were used to keep the field strength as high as possible during casting. Using 25-mm sample mold cups allowed for a magnetic field strength of approximately 1.8 T, which was measured using probes during the casting and orientation step. Due to the poor results of alignment through the epoxy casting method, further slip- and gel-casting experiments were not undertaken.

## 4.2 Problems Encountered

A number of issues were encountered that limited the positive results of this study. The major issues are presented in the following sections with brief discussions to how these issues could be overcome in future trials.

### 4.2.1 Magnet Strength

Based on background research performed prior to this investigation, it was known that a very strong magnetic field ( $\geq 10$  T) was necessary to obtain a large degree of alignment for the  $\text{Si}_3\text{N}_4$  grains. While a magnet of this strength was not available, the experiments performed as part of this study were intended to be used as preliminary tests to prove the idea and methodology further before seeking a stronger magnetic source. As stated, the maximum field strength noted during these experiments was 1.8 T, over five times lower than seen for large-scale orientation in literature papers. This may have been a large impediment for garnering en masse grain orientation for this set of experiments.

Some other options that might have helped this proof-of-concept study would have been the use of a heat-activated hardener or a wax matrix within which to conduct the powder alignment. In these cases the alignment time can be accurately controlled, unlike using epoxy where the cure time is determined by the epoxy and influenced by the curing environment.

Another important factor that may have played a role in this study is the effect of external fields possibly influencing the overarching results. An isolated chamber would be the best environment to conduct such experiments, which can be difficult in large laboratory facilities where many pieces of equipment lie in the immediate vicinity of the magnet, as well as the electromagnetic fields due to the power lines running throughout the facility floors, walls, and ceiling.

### 4.2.2 Starting Powder Morphology

Another major issue facing this study was the morphology of the starting powders.  $\text{Si}_3\text{N}_4$  powders of the  $\beta$  structure with very high aspect ratios were desired to gain the largest amount of grain orientation. However, the powders acquired for this study had a bimodal grain size distribution. The powders were purchased in a -325 mesh quantity ( $< 44 \mu\text{m}$ ); however, the grains were measured to have an order of magnitude difference between the two grain sizes (approximately 1 and 10  $\mu\text{m}$ ). The grains also did not have a very high aspect ratio; they were more spherical than rod-like. Microstructural images showing the powder morphology are presented in Fig. 3.

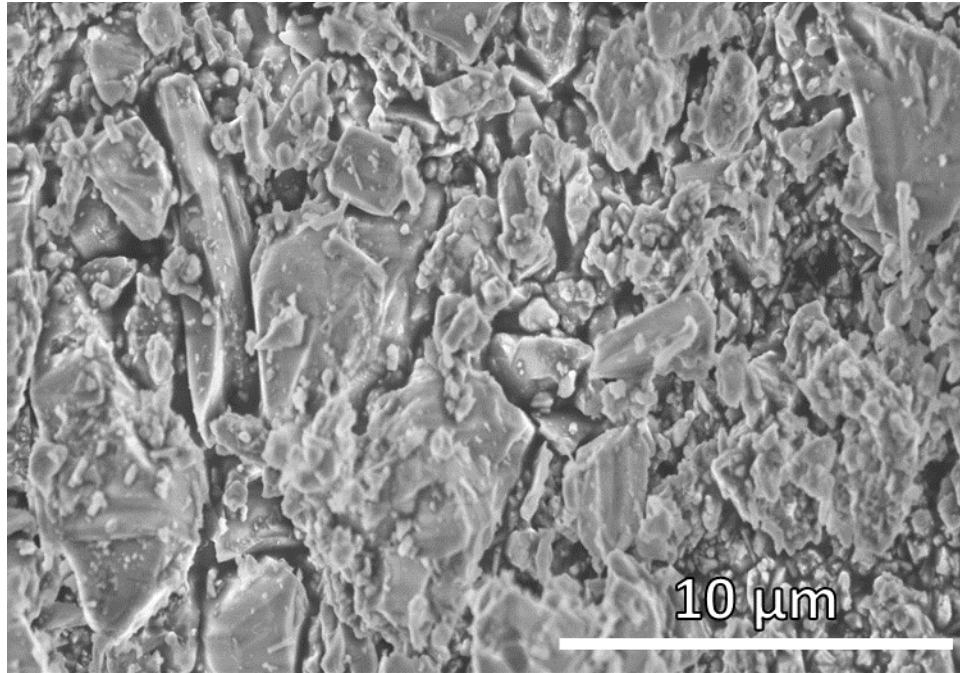


**Fig. 3 SEM image of the initial Si<sub>3</sub>N<sub>4</sub> powder**

The effect of various rare-earth oxides on the morphology of the better grains has been examined and is known to have a large influence on the resultant properties of the body. Because of the spheroid nature of the particles, the full benefits of microstructural texturing would not have been realized in any case.

#### **4.2.3 Anisotropic Magnetic Susceptibility of Silicon Nitride**

The final inhibitor for alignment is the anisotropic magnetic susceptibility of  $\beta$ -silicon nitride grains. It is known that the magnetic susceptibility, a measure of whether a material is attracted into or repelled from a magnetic field, of the c-axis is less than the susceptibility of the a and b axes (i.e.,  $\chi_c < \chi_{a,b}$ ). This behavior makes it difficult to achieve 1-axis orientation in  $\beta$ -silicon nitride, as the a- and b-axes will align in a direction, resulting in the c-axis of each grain lying in the same plane but not along the same axis. Hence, for a complete 1-axis orientation, another method may be necessary. This behavior is illustrated in Fig. 4.

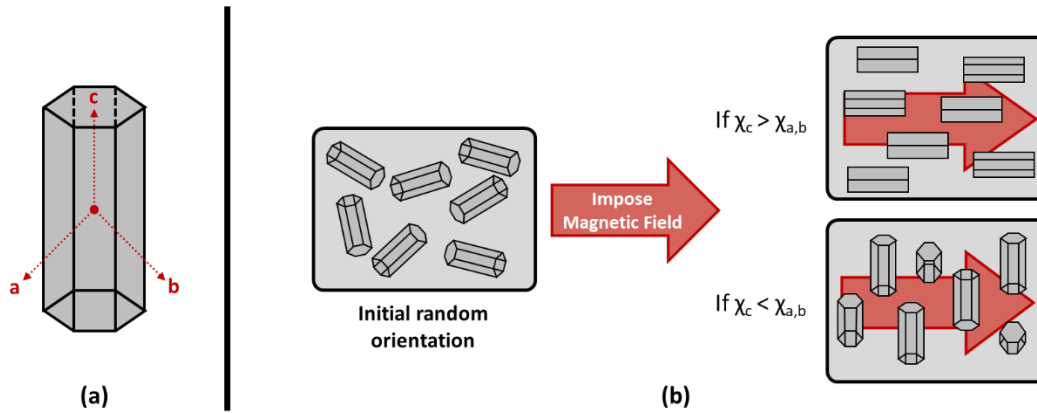


Fig. 4 a) Schematic of the hexagonal crystal of  $\beta$  silicon nitride grains with the major axes noted. b) Schematic of how the anisotropic magnetic susceptibility of  $\beta$ -silicon nitride grains affects the alignment after a magnetic field has been imposed. Because the c-axis susceptibility is below that of the a- and b-axes in silicon nitride, the particles will only align in the same plane, but not along the same direction.

## 5. Future Efforts

### 5.1 Magnetic Field Considerations

The most important factor to aid in alignment is magnetic strength; therefore, a magnetic with a much stronger maximum strength would be required to produce a better outcome. It is reported that 10 T is suitable to achieve c-axis orientation of  $\text{Si}_3\text{N}_4$ . The relationship between magnetic field strength and level of grain orientation is unknown, but it is an important parameter to consider when performing this type of experiment. However, it is supposed that a higher strength magnetic may help accomplish this result in a shorter amount of time.

Another important parameter to consider is the state of the magnetic field: static versus rotating. A static field is most useful for materials that have 1 axis of magnetic susceptibility. In the case of  $\beta$  silicon nitride, not only do all three axes exhibit susceptibility, but the a and b axes show increased behavior compared with the c-axis. As mentioned, this results in the c-axis of each grain lying within the same plane but on the same axis. Therefore, a rotating field may help to improve the alignment of the c-axis of each grain.

### 5.2 Starting Powders

As mentioned previously and presented in Fig. 3, the morphology of the starting  $\beta$   $\text{Si}_3\text{N}_4$  powders was not optimal to achieve the best levels of c-axis orientation. Beginning the experiments with higher aspect ratio starting powders (i.e., needle-like) would aid in obtaining a more textured microstructure than the spheroidal grains can provide.

### 5.3 Alternative Processing Methods

Hot pressing is a processing technique commonly employed to promote densification of  $\text{Si}_3\text{N}_4$  ceramics. However, this can become problematic due to the dissociation of silicon and nitrogen at  $1850\text{ }^\circ\text{C}$ , below the melting temperature of silicon nitride ( $1900\text{ }^\circ\text{C}$ ).<sup>29</sup> This issue can be overcome through the use of sintering additives that melt at lower temperatures to induce liquid-phase sintering, while simultaneously stimulating texture development via promotion of the  $\alpha$ -to- $\beta$  phase transformation. Hot pressing is considered a hot working technique, meaning that the development of texture is primarily through the rotation of the elongated  $\beta$  grains into the plane of pressing by the uniaxial stresses imposed upon the material rather than large-scale grain growth, as shown in Fig. 5a. On the other hand, in pressureless sintering of  $\text{Si}_3\text{N}_4$  (Fig. 5b), the texture is developed through templated grain growth due to the presence of a glassy phase. Yet both of these techniques generally only result in a material where the c-axis of the  $\beta$  grain is parallel to the plane of hot pressing or grain growth, respectively, and not in a specific direction within that plane. The potential combination of a magnetic field during hot pressing could overcome this obstacle and further facilitate the alignment of the c-axes in a given plane and preferred direction.

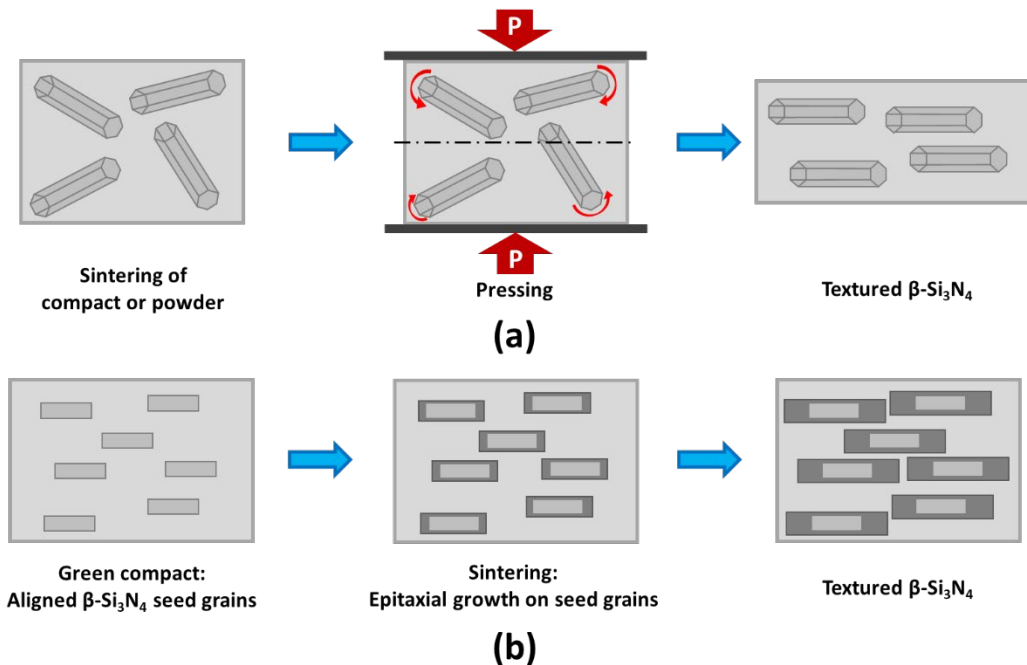


**Fig. 5** Rotation of grains due to a) hot-working and b) templated grain growth. In hot-working, the grains are aligned due to the pressing forces applied during processing; however, in templated grain growth, seed grains are aligned and then proceed to grow epitaxially during sintering to produce the large-scale microstructural texturing.

Recently there has been a large research thrust into the field of field-assisted sintering, similar to the techniques employed in the field-assisted sintering technique (FAST). This method has been utilized to produce dense  $\text{Si}_3\text{N}_4$  ceramics, but grain orientation and alignment due to this procedure has not been extensively explored. Similar to the suggestion of incorporating a field during hot pressing, the inclusion of an electromagnetic or magnetic field during FAST could assist in the alignment of  $\beta$  grains in a specific direction.

Two other possible avenues for processing textured  $\text{Si}_3\text{N}_4$  are extrusion and tape casting, as shown in Figs. 6a and 6b, respectively. Both techniques begin with a slurry containing suspended ceramic particles that is formed into a green body of a desired shape via shear forces. The green bodies can then be stacked/arranged into a larger part that is then densified through sintering/firing.

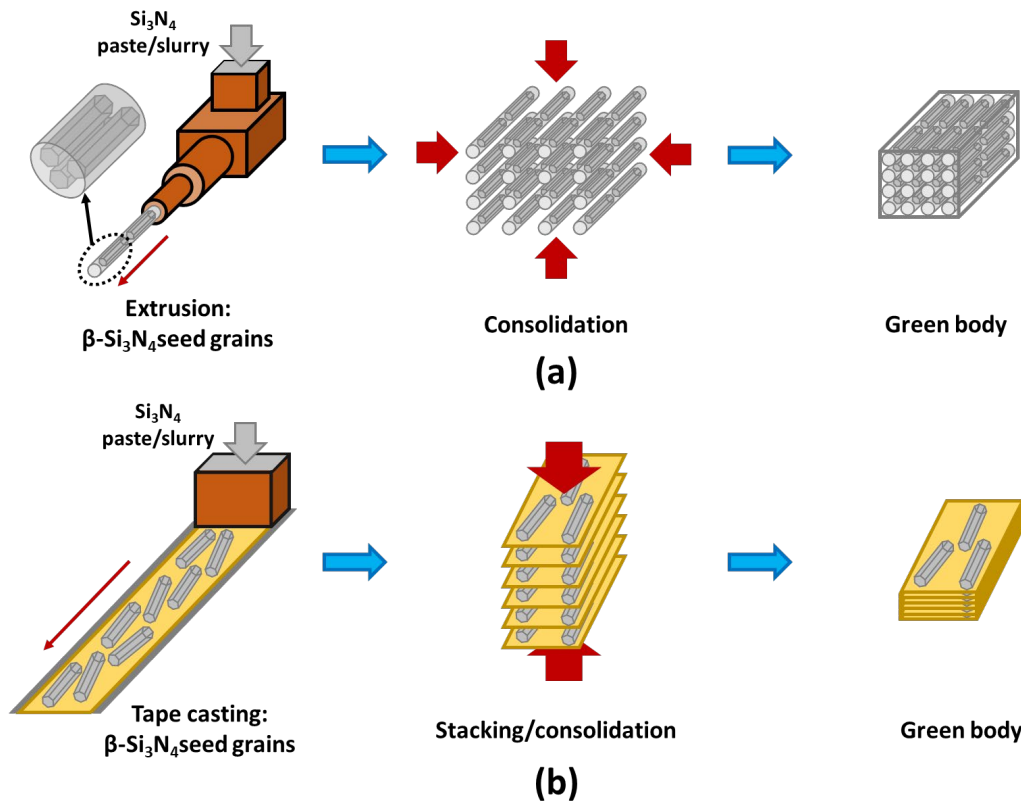


**Fig. 6** Illustrations showing how a) extrusion and b) tape casting can be utilized to produce green bodies with microstructural texturing of  $\beta$  silicon nitride grains. In extrusion, the particles are aligned in the same direction; however, in tape casting, the particles will lie in the same plane but not all pointing in the same direction.

Tape casting creates a green sheet with oriented anisotropic grains by casting the slurry onto a substrate through a doctor blade that levels the slurry. These sheets can be stacked to form a larger green body for sintering. Extrusion relies on shear forces generated at the outlet die of the extruding machine to induce the grain

rotation and alignment. Both of these techniques result in a body with an extremely high degree of  $\beta$  grain alignment in the cast/extruded direction. Both techniques are highly dependent upon the amount of shear strain developed during the process. Extrusion is typically performed with highly viscous suspensions and at higher rates than tape casting. This leads to an increased amount of shear during processing, resulting in better alignment from extrusion as opposed to tape casting. However, additional modifications to the tape casting method can help improve the alignment of the whisker-like grains.

#### **5.4 Controlling Grain Orientation for Specific Applications**

---

The ability to control the grain orientation for a specific application could be extremely useful in many instances. For example, some applications may desire a very highly oriented microstructure, as the imposed stress-field and crack direction may always lie in a direction perpendicular to the c-axis of the material. Computer modeling of the exact process may be beneficial when engineering these materials for a designated application. Depending upon the imposed stress field and corresponding crack direction, alignment along an axis, plane, or 3-D surface or direction may be required to increase the fracture toughness of the part and, hopefully, prolong the life of the part.

This ideology could be further expanded using a process referred to as “3-D magnetic printing”, as shown in Fig. 7. The work in Martin et al.<sup>30</sup> on this subject was inspired by biological materials that have elaborate reinforcement and texturing patterns. By following the process outlined in Fig. 7, custom-designed texturing can be generated in a material through a layer-by-layer powder deposition process, where each layer undergoes alignment and then selective areas are frozen in place through UV light exposure. The magnetic field is then shifted in another direction allowing the nonfrozen areas to be re-aligned in this new direction. This concept could be expanded to ceramics that are magnetically susceptible, such as  $\beta$ - $\text{Si}_3\text{N}_4$ , to produce highly textured microstructures that can be customized and engineered for a desired application.

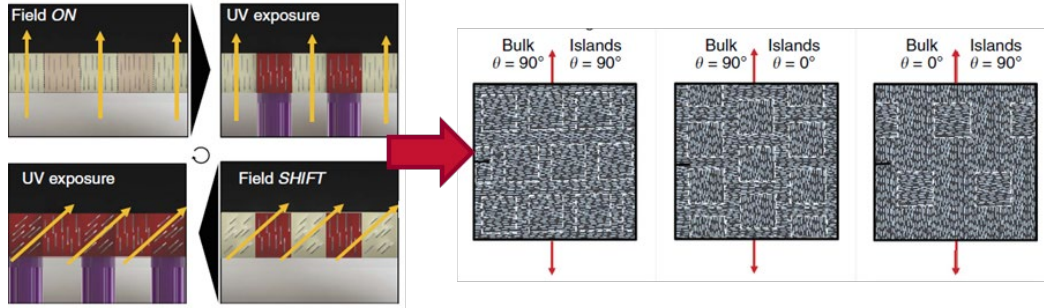


**Fig. 7** Illustration of how 3-D magnetic printing can be used to produce ceramics with highly controllable microstructural texturing. Through selective sintering and alignment procedures, different regions or layers of material can be oriented in their own independent direction, resulting in a material with an enhanced, but exceedingly controlled, microstructural texturing. (Image reprinted with permission from Martin et al.<sup>31</sup>)

## 6. References

---

1. Riley FL. Silicon nitride and related materials. *Journal of the American Ceramic Society*. 2000;83(2):245–265.
2. Ziegler G, Heinrich J, Wötting G. Relationships between processing, microstructure and properties of dense and reaction-bonded silicon nitride. *Journal of Materials Science*. 1987;22(9):3041–3086.
3. Zhu X, Sakka Y. Textured silicon nitride: processing and anisotropic properties. *Sci Technol Adv Mater*. 2008;9(3):033001.
4. Teshima H, Hirao K, Toriyama M, Kanzaki S. Fabrication and mechanical properties of silicon nitride ceramics with unidirectionally oriented rodlike grains. *Journal of the Ceramic Society of Japan*. 1999;107(1252):1216–1220.
5. Nakamura M, Hirao K, Yamauchi Y, Kanzaki S. Tribological properties of unidirectionally aligned silicon nitride. *Journal of the American Ceramic Society*. 2001;84(11):2579–2584.
6. Santos C, Strecker K, Baldacim SA, da Silva OMM, da Silva CRM. Influence of additive content on the anisotropy in hot-pressed  $\text{Si}_3\text{N}_4$  ceramics using grain orientation measurements. *Ceramics International*. 2004;30(5):653–659.
7. Belmonte M, Miranzo P, Osendi M. Mechanical properties and contact damage behavior in aligned silicon nitride materials. *Journal of the American Ceramic Society*. 2007;90(4):1157–1163.
8. Goto Y HO, Ohta H, Komatsu M, Komeya K. Preferred orientation and mechanical properties of pressureless sintered silicon nitride. *Journal of the Ceramic Association of Japan*. 1986;94(1085):177–181.
9. Kawashima T, Okamoto H, Yamamoto H, Kitamura A. Grain size dependence of the fracture toughness of silicon nitride ceramics. *Journal of the Ceramic Society of Japan*. 1991;99(1148):320–323.
10. Hirosaki N, Akimune Y, Mitomo M. Effect of grain growth of  $\beta$ -silicon nitride on strength, Weibull modulus, and fracture toughness. *Journal of the American Ceramic Society*. 1993;76(7):1892–1894.
11. Björklund H, Falk LK. Grain morphology and intergranular microstructure of whisker reinforced  $\text{Si}_3\text{N}_4$  ceramics. *Journal of the European Ceramic Society*. 1997;17(1):13–24.
12. Becher PF, Sun EY, Plucknett KP, Alexander KB, Hsueh C-H, Lin H-T, Waters SB, Westmoreland CG, Kang E-S, Hirao K, Brito ME. Microstructural

- design of silicon nitride with improved fracture toughness: I. effects of grain shape and size. *Journal of the American Ceramic Society*. 1998;81(11):2821–2830.
13. Peillon FC, Thevenot F. Microstructural designing of silicon nitride related to toughness. *Journal of the European Ceramic Society*. 2002;22(3):271–278.
  14. Hirao K, Nagaoka T, Brito ME, Kanzaki S. Microstructure control of silicon nitride by seeding with rodlike  $\beta$ -silicon nitride particles. *Journal of the American Ceramic Society*. 1994;77(7):1857–1862.
  15. Sun EY, Becher PF, Plucknett KP, Hsueh C-H, Alexander KB, Waters SB, Hirao K, Brito ME. Microstructural design of silicon nitride with improved fracture toughness: II. effects of yttria and alumina additives. *Journal of the American Ceramic Society*. 1998;81(11):2831–2840.
  16. Hirao K, Ohashi M, Brito ME, Kanzaki S. Processing strategy for producing highly anisotropic silicon nitride. *Journal of the American Ceramic Society*. 1995;78(6):1687–1690.
  17. Kondo N, Suzuki Y, Ohji T. Superplastic sinter-forging of silicon nitride with anisotropic microstructure formation. *Journal of the American Ceramic Society*. 1999;82(4):1067–1069.
  18. Li S, Sassa K, Asai S. Fabrication of textured  $\text{Si}_3\text{N}_4$  ceramics by slip casting in a high magnetic field. *Journal of the American Ceramic Society*. 2004;87(7):1384–1387.
  19. Mikijelj B, Nawaz Z. Improved  $\text{Si}_3\text{N}_4$  material for gun barrel applications: phase 4. Aberdeen Proving Ground (MD): Army Research Laboratory (US): 2013 June. Report No.: ARL-CR-715.
  21. Mikijelj B, Nawaz Z. Improved  $\text{Si}_3\text{N}_4$  material for gun barrel applications final report: phase 1, year 1. Aberdeen Proving Ground (MD): Army Research Laboratory (US): 2010 Aug. Report No.: ARL-CR-653.
  22. Mikijelj B, Nawaz Z. Improved  $\text{Si}_3\text{N}_4$  material for gun barrel applications: phase 2. Aberdeen Proving Ground (MD): Army Research Laboratory (US): 2011 Nov. Report No.: ARL-CR-682.
  23. Mikijelj B, Nawaz Z. Improved  $\text{Si}_3\text{N}_4$  material for gun barrel applications: phase 3. Aberdeen Proving Ground (MD): Army Research Laboratory (US): 2012 Aug. Report No.: ARL-CR-699.

24. Jiang J, Kragh F, Frost DJ, Stahl K, Lindelov H. Hardness and thermal stability of cubic silicon nitride. *Journal of Physics: Condensed Matter*. 2001;13(22):L515.
25. Yang Z, Yu J, Deng K, Lan L, Wang H, Ren Z, Wang Q, Dai Y, Wang H. Fabrication of textured Si<sub>3</sub>N<sub>4</sub> ceramics with β-Si<sub>3</sub>N<sub>4</sub> powders as raw material by gel-casting under strong magnetic field. *Materials Letters*. 2014;135:218–221.
26. Guo W-M, Yu J-J, Xiong M, Lin H-T. High-toughness Lu<sub>2</sub>O<sub>3</sub>-doped Si<sub>3</sub>N<sub>4</sub> ceramics by seeding. *Ceramics International*. 2016;42(5):6495–6499.
27. Becher PF, Painter GS, Shibata N, Waters SB. Effects of rare-earth (RE) intergranular adsorption on the phase transformation, microstructure evolution, and mechanical properties in silicon nitride with RE<sub>2</sub>O<sub>3</sub> + MgO additives: RE=La, Gd, and Lu. *Journal of the American Ceramic Society*. 2008;91(7):2328–2336.
28. Satet RL, Hoffmann MJ. Influence of the rare-earth element on the mechanical properties of RE–Mg-bearing silicon nitride. *Journal of the American Ceramic Society*. 2005;88(9):2485–2490.
29. Furushima R, Tanaka S, Kato Z, Uematsu K. Orientation distribution—Lotgering factor relationship in a polycrystalline material—as an example of bismuth titanate prepared by a magnetic field. *Journal of the Ceramic Society of Japan*. 2010;118(1382):921–926.
30. Li S, Wu C, Sassa K, Asai S. The control of crystal orientation in ceramics by imposition of a high magnetic field. *Materials Science and Engineering: A*. 2006;422(1-2):227–231.
31. Haynes WM. *CRC handbook of chemistry and physics*. Boca Raton (FL): CRC Press; 2014.
32. Martin JJ, Fiore BE, Erb RM. Designing bioinspired composite reinforcement architectures via 3D magnetic printing. *Nature Communications*. 2015;6.

## List of Symbols, Abbreviations, and Acronyms

---

3-D	three-dimensional
$\alpha$	alpha
A	aligned specimen
ARL	Army Research Laboratory
AS	aligned and sintered specimen
$\beta$	beta
C	control specimen
FAST	field-assisted sintering technique
$\gamma$	gamma
<i>LF</i>	Lotgering factor
PDF	powder diffraction file
SEM	scanning electron microscopy
Si <sub>3</sub> N <sub>4</sub>	silicon nitride
UV	ultraviolet
XRD	X-ray diffraction

1 DEFENSE TECHNICAL  
(PDF) INFORMATION CTR  
DTIC OCA

1 CCDC ARL  
(PDF) FCDD RLD CL  
TECH LIB

1 GOVT PRINTG OFC  
(PDF) A MALHOTRA

1 CCDC ARL  
(PDF) FCDD RLW MB  
J PITTARI